

Double-layered distributed transient frequency control with regional coordination for power networks

Yifu Zhang and Jorge Cortés

Abstract—This paper proposes a control strategy for power systems with a two-layer structure that achieves global stabilization and, at the same time, delimits the transient frequencies of targeted buses to a desired safe interval. The first layer is a model predictive control that, in a receding horizon fashion, optimally allocates the power resources while softly respecting transient frequency constraints. As the first layer control requires solving an optimization problem online, it only periodically samples the system state and updates its action. The second layer control, however, is implemented in real time, assisting the first layer to achieve frequency invariance and attractivity requirements. We show that the controllers designed at both layers are Lipschitz in the state. Furthermore, through network partition, they can be implemented in a distributed fashion, only requiring system information from neighboring partitions. Simulations on the IEEE 39-bus network illustrate our results.

I. INTRODUCTION

Power network frequency is used as a key performance metric in designing load shedding scheme [1]. In simulations, such a frequency refers to the system frequency that reflects the weighted average frequencies of all synchronous generators; however, in practice, due to the lack of availability of measurements for all generators, only a few of them are selected and sampled for monitoring and control design [2]. Furthermore, from the point of view of contingency recovery, even if the power supply and demand are re-balanced after a failure, due to the interconnected dynamics and inertia of power networks, individual buses may still be isolated from the network due to overheating relay protection. Therefore, there is a need of designing control schemes to restrict single bus transient frequency to evolve within an allowable range under disturbances and contingencies. This is the problem we address in this paper, paying special attention to the distributed implementation of the controller as well as the reduction of the control effort through cooperation.

Literature review: Literature [3], [4] proposes several sufficient conditions on power network synchronization; however, as they do not consider bus transient frequency limit as a constraint, the ideal synchronization condition may not hold due to possible violation in frequency transients. Work [5] studies the relation between power injection disturbance and frequency overshoot of individual bus without active control to regulate frequency transients. On the other hand, to actively control power network transients, several strategies have been investigated, including inertial placement [6], power system stabilizer [7], and power supply re-allocation [8]. Yet, these

strategies, aiming at improving system transient behaviors, cannot rigorously constrain the evolution of frequency to stay within a safe region. In this regard, we propose two different control frameworks [9], [10] to achieve both synchronization and frequency safety. Specifically, as opposed to that in [9], control strategy in [10] enables cooperation among neighboring buses and reduces the overall control effort in a receding horizon fashion through solving an optimization problem to seek for the optimal control trajectory. However, this ideal control framework faces practical challenges from two aspects in real-time implementation. First, it generally takes a long period of time to find the optimal control trajectory. Second, the control framework requires finding such an optimal control trajectory at every time instant. These deficiencies motivate us to design another framework that can be implemented in real-time while maintaining the advantage of cooperation.

Statement of contribution: This paper proposes a control strategy that achieves the following requirements through a dynamical state-feedback control design: (i) The closed-loop system is asymptotically stable. (ii) For every targeted bus, under perturbation from power injections or network dynamical interactions, its whole frequency trajectory stays within a given safe region, provided its initial frequency lies in the same region. (iii) If this is not the case, then the frequency trajectory should enter the safe region within a finite time and never leaves it afterwards. (iv) The control strategy is distributed by only requiring local state and network information. Hereby, we propose a double-layered control structure, where the second layer control strategy is similar to that in [10]; however, by relaxing the frequency constraints and restricting the possible control trajectory from arbitrary to constant signal, the second-layer controller only needs to periodically (as opposed to continuously) solve an optimal control trajectory, and the time consumption for seeking the optimal one is greatly reduced and almost negligible. The first layer controller, coming from [9], only slightly tunes the output of the second layer control signal so that the overall signal rigorously ensures requirement (i)-(iv). We also show that the proposed control is Lipschitz in state and continuous in time. We verify our results on the IEEE 39-bus power network.

II. PRELIMINARIES

We introduce here notation and notions from graph theory.

Notation: Let \mathbb{N} , \mathbb{R} , $\mathbb{R}_{>}$, and \mathbb{R}_{\geq} denote the set of natural, real, positive real, and nonnegative real numbers, respectively. Variables are assumed to belong to the Euclidean space if not specified otherwise. Denote $\mathbf{1}_n$ and $\mathbf{0}_n$ in \mathbb{R}^n

The authors are with the Department of Mechanical and Aerospace Engineering, University of California, San Diego, CA 92093, USA, {yifuzhang, cortes}@ucsd.edu

as the vector of all ones and zeros, resp. For $a \in \mathbb{R}$, $\lceil a \rceil$ denote its ceiling. We let $\|\cdot\|$ denote the 2-norm on \mathbb{R}^n . For a vector $b \in \mathbb{R}^n$, b_i denotes its i th entry. For $A \in \mathbb{R}^{m \times n}$, let $[A]_i$ and $[A]_{i,j}$ denote its i th row and (i,j) th element, resp. For any $c, d \in \mathbb{N}$, let $[c, d]_{\mathbb{N}} = \{x \in \mathbb{N} | c \leq x \leq d\}$. Denote the sign function $\text{sgn} : \mathbb{R} \rightarrow \{0, 1\}$ as $\text{sgn}(a) = 1$ if $a \geq 0$, and as $\text{sgn}(a) = -1$ if $a < 0$. Finally, denote the saturation function $\text{sat} : \mathbb{R} \rightarrow \mathbb{R}$ with limits $a^{\min} < a^{\max}$ by $\text{sat}(a; a^{\max}, a^{\min}) = a^{\max}$ if $a \geq a^{\max}$, $\text{sat}(a; a^{\max}, a^{\min}) = a^{\min}$ if $a \leq a^{\min}$, and $\text{sat}(a; a^{\max}, a^{\min}) = a$ otherwise.

Algebraic graph theory: We employ basic notions in algebraic graph theory, cf. [11], [12]. An undirected graph is a pair $\mathcal{G} = (\mathcal{S}, \mathcal{E})$, where $\mathcal{S} = \{1, \dots, n\}$ is the vertex set and $\mathcal{E} = \{e_1, \dots, e_m\} \subseteq \mathcal{S} \times \mathcal{S}$ is the edge set. An induced subgraph $\mathcal{G}_\beta = (\mathcal{S}_\beta, \mathcal{E}_\beta)$ of $\mathcal{G} = (\mathcal{S}, \mathcal{E})$ satisfies $\mathcal{S}_\beta \subseteq \mathcal{S}$, $\mathcal{E}_\beta \subseteq \mathcal{E}$, and $(i, j) \in \mathcal{E}_\beta$ if $(i, j) \in \mathcal{E}$ with $i, j \in \mathcal{S}_\beta$. Additionally, $\mathcal{E}_\beta^t \subseteq \mathcal{S}_\beta \times (\mathcal{S} \setminus \mathcal{S}_\beta)$ denotes the collection of edges connecting \mathcal{G}_β and the rest of the network. A path is an ordered sequence of vertices such that any pair of consecutive vertices in the sequence is an edge of the graph. A graph is connected if there exists a path between any two vertices. Two nodes are neighbors if there exists an edge linking them. Denote $\mathcal{N}(i)$ as the set of neighbors of node i . For each edge $e_k \in \mathcal{E}$ with vertices i, j , an orientation consists of choosing either i or j to be the positive end of e_k and the other vertex to be the negative end. The incidence matrix $D = (d_{ki}) \in \mathbb{R}^{m \times n}$ associated with \mathcal{G} is defined as $d_{ki} = 1$ if i is the positive end of e_k , $d_{ki} = -1$ if i is the negative end of e_k , and $d_{ki} = 0$ otherwise.

III. PROBLEM STATEMENT

In this section we introduce the dynamics of the power network and the control requirements.

A. Power network model

The power network is modeled by a connected undirected graph $\mathcal{G} = (\mathcal{S}, \mathcal{E})$, where $\mathcal{S} = \{1, 2, \dots, n\}$ stands for the collection of buses (nodes) and $\mathcal{E} = \{e_1, e_2, \dots, e_m\} \subseteq \mathcal{S} \times \mathcal{S}$ represents the collection of transmission lines (edges). For every bus $i \in \mathcal{S}$, let $\omega_i \in \mathbb{R}$, $p_i \in \mathbb{R}$, $M_i \in \mathbb{R}_{\geq}$, and $E_i \in \mathbb{R}_{\geq}$ denote the nodal information of shifted voltage frequency relative to the nominal frequency, active power injection, inertial, and damping coefficient, respectively. For simplicity, we assume that the latter two are strictly positive. Given an arbitrary orientation on \mathcal{G} , for any edge with positive end i and negative end j , let f_{ij} be its signed power flow and $b_{ij} \in \mathbb{R}_{>}$ the line susceptance. Let $\mathcal{S}^u \subset \mathcal{S}$ be the collection of buses with exogenous control inputs. To stack this notation in a more compact way, let $f \in \mathbb{R}^m$, $\omega \in \mathbb{R}^n$ and $p \in \mathbb{R}^n$ denote the collection of f_{ij} 's, ω_i 's, and p_i 's, resp. Let $Y_b \in \mathbb{R}^{m \times m}$ be the diagonal matrix whose k th diagonal entry is the susceptance of the transmission line e_k connecting i and j , i.e., $[Y_b]_{k,k} = b_{ij}$. Let $M \triangleq \text{diag}(M_1, M_2, \dots, M_n) \in \mathbb{R}^{n \times n}$, $E \triangleq \text{diag}(E_1, E_2, \dots, E_n) \in \mathbb{R}^{n \times n}$, and $D \in \mathbb{R}^{m \times n}$ be the incidence matrix. The linearized network dynamics is [13], [14],

$$\dot{f}(t) = Y_b D \omega(t), \quad (1a)$$

$$M \dot{\omega}(t) = -E \omega(t) - D^T f(t) + p(t) + \alpha(t), \quad (1b)$$

where $\alpha(t) \in \mathbb{A} \triangleq \{y \in \mathbb{R}^n | y_w = 0 \text{ for } w \in \mathcal{S} \setminus \mathcal{S}^u\}$. For convenience, we use $x \triangleq (f, \omega) \in \mathbb{R}^{m+n}$. We adopt the following assumption on the power injections.

Assumption 3.1: (Finite-time convergence of active power injection). For each $i \in \mathcal{S}$, p_i is piece-wise continuous and becomes constant (denoted by p_i^*) after a finite time, i.e., there exists $0 \leq \bar{t} < \infty$ such that $p_i(t) = p_i^*$ for every $i \in \mathcal{S}$ and every $t \geq \bar{t}$. Furthermore, the constant power injections are balanced, i.e., $\sum_{i \in \mathcal{S}} p_i^* = 0$.

Note that Assumption 3.1 generalizes the power injection profile from the commonly used time-invariant case (e.g. [15], [16]) to the finite-time convergent case. Also, as our controller design here lies in the scope of primary and secondary control, we assume that the power injection designed by the tertiary control through economic dispatch is balanced after a finite time. Under Assumption 3.1, one can show [9] that, for the open-loop system (i.e., (1) with $\alpha \equiv \mathbf{0}_n$), the trajectories $(f(t), \omega(t))$ globally converges to the unique equilibrium point $(f_\infty, \mathbf{0}_n)$, where f_∞ is uniquely determined by the power injection profile and network parameters.

B. Control requirements

Our goal is to design distributed state-feedback controllers, one per each bus $i \in \mathcal{S}^u$, which maintain stability of the power network while at the same time cooperatively guaranteeing frequency invariance and attractivity of nodes in a targeted subset \mathcal{S}^ω of \mathcal{S}^u . Formally, the designed closed-loop system should meet the following requirements.

(i) *Frequency invariance:* For each $i \in \mathcal{S}^\omega$, let $\underline{\omega}_i \in \mathbb{R}$ and $\bar{\omega}_i \in \mathbb{R}$ be lower and upper safe frequency bounds, with $\underline{\omega}_i < \bar{\omega}_i$. The trajectory of ω_i must stay inside $[\underline{\omega}_i, \bar{\omega}_i]$, provided that its initial frequency $\omega_i(0)$ lies inside $[\underline{\omega}_i, \bar{\omega}_i]$. This requirement guarantees that every targeted frequency always evolves inside the safe region.

(ii) *Frequency attractivity:* For each $i \in \mathcal{S}^\omega$, if $\omega_i(0) \notin [\underline{\omega}_i, \bar{\omega}_i]$, then there exists a finite time t_0 such that $\omega_i(t) \in [\underline{\omega}_i, \bar{\omega}_i]$ for every $t \geq t_0$. This requirement guarantees safe recovery from an undesired initial frequency.

(iii) *Asymptotic stability:* The controller should only regulate the system's transients, i.e., the closed-loop system should globally converge to the same equilibrium point $(f_\infty, \mathbf{0}_n)$ of the open-loop system.

(iv) *Lipschitz continuity:* The controller must have Lipschitz in its state argument. This suffices to ensure the existence and uniqueness of solution for the closed-loop system and, furthermore, guarantees that the control action is robust to state measurement errors.

(v) *Economic cooperation:* The individual controllers α_i , $i \in \mathcal{S}^u$, should cooperate with each other to reduce the overall control effort measure by two norm.

(vi) *Distributed nature:* Every individual controller can only utilize the state and power injection information within a local region designed by operator. This reflects a practical requirement for implementation in larger-scale power networks, in which case centralized control strategies depending on global information may face critical challenge for real-time execution.

IV. CENTRALIZED DOUBLE-LAYERED CONTROLLER

In this section, we introduce a centralized controller that achieves the requirements (i)-(v) identified in Section III-B. Based on this design, we later propose a distributed version that also achieves requirement (vi).

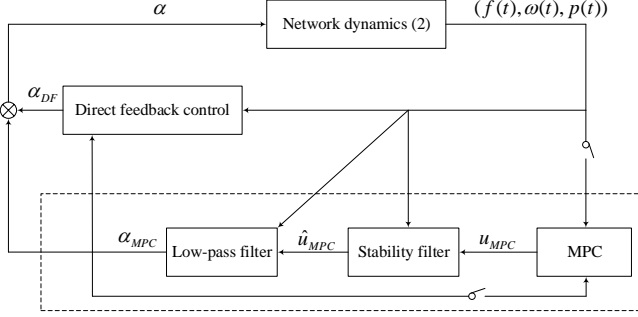


Fig. 1. Block diagram of the closed-loop system.

We adopt the centralized control structure depicted in Figure 1. The control signal α consists of two parts

$$\alpha = \alpha_{DF} + \alpha_{MPC}. \quad (2)$$

We next describe the role played by each part. The bottom layer solves an optimization problem online. To do so, it combines an MPC component cascaded with a stability filter and a low-pass filter. The MPC component periodically and optimally allocates control resources, while roughly adjusting the frequency trajectories as a first step to achieve frequency invariance and attractivity. Its output is designed to be a piece-wise constant signal u_{MPC} , which becomes a piece-wise continuous signal \hat{u}_{MPC} after passing through the stability filter. The low-pass filter ensures that the output α_{MPC} of the bottom layer control is continuous in time to avoid any discontinuous change in control signal. Using real-time state information, the stability filter guarantees that α_{MPC} does not jeopardize system stability. The bottom layer controller achieves economic cooperation and stabilization, but does not guarantee frequency invariance and attractivity. The top layer controller is called direct feedback control since, unlike the bottom layer control, can be directly computed in real time. This layer slightly modifies the control generated by the bottom layer to ensure frequency invariance and attractivity while maintaining stability of the system.

A. Bottom layer controller design via MPC and filters

Here we formally describe each component in the bottom layer control and analyze their properties.

1) *MPC component*: The MPC component operates on a periodic time schedule. In each sampling period, the MPC component aims to allocate control resources over controlled nodes in an open-loop fashion based on the latest sampling system state and forecasted power injection. Here, due to the additional dynamics of the low-pass filter, the system state consists of not only power network state (f, ω) , but also the state of low pass filter α_{MPC} that we later explain. Formally, let $\{\Delta^j\}_{j \in \mathbb{N}}$ be the collection of sampling points. At time

$t = \Delta^j$, let a piece-wise continuous signal $p_t^{fcst} : [t, t + \tilde{T}] \rightarrow \mathbb{R}^n$ be the forecasted value of the power injection p for the first \tilde{T} seconds after t . We discretize the dynamics (1) and denote $N \triangleq \lceil \tilde{T}/T \rceil$ as the length of the predicted step with some $T > 0$. At each $t = \Delta^j$, the MPC component updates its output by solving the following optimization problem,

$$\begin{aligned} \min_{\hat{F}, \hat{\Omega}, \hat{A}, \hat{u}, \beta} \quad & g(\hat{u}, \beta) \triangleq \sum_{i \in \mathcal{S}^u} c_i \hat{u}_i^2 + d\beta^2 \\ \text{s.t.} \quad & \hat{f}(k+1) = \hat{f}(k) + TY_b D \hat{\omega}(k), \\ & M \hat{\omega}(k+1) = M \hat{\omega}(k) + T \{ -E \hat{\omega}(k) - D^T \hat{f}(k) + \\ & \quad \hat{p}^{fcst}(k) + \hat{u} \}, \forall k \in [0, N-1]_{\mathbb{N}}, \quad (3a) \\ & \hat{\alpha}_i(k+1) = \hat{\alpha}_i(k) + T \{ -\hat{\alpha}_i(k)/T_i - \hat{\omega}_i(k) + \hat{u}_i \}, \forall i \in \mathcal{S}^u, \\ & \hat{\alpha}_i \equiv 0, \quad \forall i \in \mathcal{S} \setminus \mathcal{S}^u, \quad (3b) \\ & \hat{u} \in \mathbb{A}, \quad (3c) \\ & \hat{f}(0) = f(\Delta^j), \quad \hat{\omega}(0) = \omega(\Delta^j), \quad \hat{\alpha}(0) = \alpha_{MPC}(\Delta^j), \quad (3d) \\ & \underline{\omega}_i - \beta \leq \hat{\omega}_i(k+1) \leq \bar{\omega}_i + \beta, \quad \forall i \in \mathcal{S}^\omega, \forall k \in [0, N-1]_{\mathbb{N}}, \quad (3e) \\ & |\hat{u}_i| \leq \varepsilon_i |\alpha_{MPC, i}(\Delta^j)|, \quad \forall i \in \mathcal{S}^u. \quad (3f) \end{aligned}$$

In this optimization problem, (3a) is the discretized dynamics corresponding to (1) via first-order discretization, and $\hat{p}^{fcst}(k) \triangleq p_{\Delta^j}^{fcst}(\Delta^j + kT)$ for every $k \in [0, N-1]_{\mathbb{N}}$; (3b) is the discretized dynamics of the low-pass filter (explained below), with $T_i > 0$ determining the filter bandwidth; (3c) indicates the availability of control signal indexes; (3d) is the initial state, where $f(\Delta^j)$, $\omega(\Delta^j)$, and $\alpha_{MPC}(\Delta^j)$ are sampled state values at time $t = \Delta^j$; (3e) represents the relaxed constraint on frequency invariance, where we allow the discretized frequency $\hat{\omega}_i$ with $i \in \mathcal{S}^\omega$ exceed its bounds $\underline{\omega}_i$ and $\bar{\omega}_i$ at the cost of a penalty term β ; (3f) bounds the control input \hat{u}_i via a coefficient $\varepsilon_i > 0$ as a function of the state of the low-pass filter to limit the sensitivity to changes in the latter; the cost function g consists of the overall control effort as well as a penalty term for frequency violation, where $c_i > 0$ for each $i \in \mathcal{S}^u$ and $d > 0$. In the above expression, we use the compact notation

$$\hat{F} \triangleq [\hat{f}(0), \hat{f}(1), \dots, \hat{f}(N)], \quad (4a)$$

$$\hat{\Omega} \triangleq [\hat{\omega}(0), \hat{\omega}(1), \dots, \hat{\omega}(N)], \quad (4b)$$

$$\hat{A} \triangleq [\hat{\alpha}(0), \hat{\alpha}(1), \dots, \hat{\alpha}(N)], \quad (4c)$$

$$\hat{p}^{fcst} \triangleq [\hat{p}^{fcst}(0), \hat{p}^{fcst}(1), \dots, \hat{p}^{fcst}(N-1)], \quad (4d)$$

as the collection of discretized state trajectories of flow, frequency, low-pass filter, and forecasted power injection.

We refer to the optimization problem (3) as $\mathbf{R}(\mathcal{G}, \mathcal{S}^u, \mathcal{S}^\omega, p_{\Delta^j}^{fcst}, f(\Delta^j), \omega(\Delta^j), \alpha_{MPC}(\Delta^j))$ to emphasize its dependence on network topology, nodal indexes with exogenous control signals, nodal indexes with transient frequency requirement, forecasted power injection, and state values at the sampling time. If the context is clear, we simply use \mathbf{R} . Let $(\hat{F}^*, \hat{\Omega}^*, \hat{A}^*, \hat{u}^*, \beta^*)$ denote its optimal solution.

Remark 4.1: (Selection of frequency violation penalty coefficient). The role of the parameter d in the objective function is to ensure that the controller that results from the MPC component does not completely disregard the frequency

invariance and attractivity requirement. In the extreme case $d = 0$ (i.e., no penalty for frequency violation), then we have $\hat{u}^* = \mathbf{0}_n$. As d grows, the resulting MPC controller ensures that violations in frequency invariance become smaller. The top layer control introduced later adds additional input to the resulting controller to ensure the frequency requirements. We come back to this point later in the simulations of Section VI.

Given the open-loop optimization problem (3), the function u_{MPC} corresponding to the MPC component in Figure 1 is defined as follows: for $j \in \mathbb{N}$ and $t \in [\Delta^j, \Delta^{j+1})$, let

$$u_{MPC}(t) = \hat{u}^*(\mathcal{G}, \mathcal{S}^u, \mathcal{S}^\omega, \hat{p}_{\Delta^j}^{fcst}, f(\Delta^j), \omega(\Delta^j), \alpha_{MPC}(\Delta^j)), \quad (5)$$

where in the right hand side we emphasize the dependence of \hat{u}^* on the seven arguments. Next, we characterize how the controller depends on the state value at the sampling time and predicted power injection.

Lemma 4.2: (Piece-wise affine and continuous dependence of optimal solution on sampling state and predicted power injection). The optimization problem $\mathbf{R}(\mathcal{G}, \mathcal{S}^u, \mathcal{S}^\omega, \hat{p}_{\Delta^j}^{fcst}, f(\Delta^j), \omega(\Delta^j), \alpha_{MPC}(\Delta^j))$ in (3) has a unique optimal solution $(\hat{F}^*, \hat{\Omega}^*, \hat{A}^*, \hat{u}^*, \beta^*)$. Furthermore, given \mathcal{G} , \mathcal{S}^u , and \mathcal{S}^ω , \hat{u}^* is a continuous and piece-wise affine in $(\hat{p}_{\Delta^j}^{fcst}, f(\Delta^j), \omega(\Delta^j), \alpha_{MPC}(\Delta^j))$, that is, there exist $l \in \mathbb{N}$, $\{H_i\}_{i=1}^l$, $\{S_i\}_{i=1}^l$, $\{h_i\}_{i=1}^l$, and $\{s_i\}_{i=1}^l$ with suitable dimensions such that

$$\hat{u}^* = S_i z + s_i, \text{ if } z \in \{y | H_i y \leq h_i\} \text{ and } i \in [1, l]_{\mathbb{N}} \quad (6)$$

holds for every $z \in \mathbb{R}^{(N+2)n+m}$, where z is the collection of $(\hat{p}_{\Delta^j}^{fcst}, f(\Delta^j), \omega(\Delta^j), \alpha_{MPC}(\Delta^j))$ in a column vector form.

Proof: We start by noting that \mathbf{R} is feasible (hence at least one optimal solution exists) for any given z . This is because, given a state trajectory $(\hat{F}, \hat{\Omega}, \hat{A})$ of (3a)-(3b) with input $\hat{u} = \mathbf{0}_n$ and initial condition (3d), choosing a sufficiently large β makes it satisfy constraint (3). The uniqueness follows from the strict convexity of g and the linearity of constraints. To show continuity and piece-wise affinity, we separately consider $2^{|\mathcal{S}^u|}$ cases, depending on the sign of each $\{\alpha_{MPC,i}(\Delta^j)\}_{i \in \mathcal{S}^u}$. Specifically, let $\eta \triangleq \{\eta_i\}_{i \in \mathcal{S}^u} \in \{1, -1\}^{|\mathcal{S}^u|}$ and define $\mathfrak{B}^\eta \triangleq \{z | (-1)^{\eta_i} \alpha_{MPC,i}(\Delta^j) \geq 0, \forall i \in \mathcal{S}^u\}$. Note that every z lies in at least one of these sets and that, in any \mathfrak{B}^η , the sign of each $\alpha_{MPC,i}(\Delta^j)$ with $i \in \mathcal{S}^u$ is fixed. Hence all the $|\mathcal{S}^u|$ constraints in (3f) can be transformed into one of the following forms

$$-\varepsilon_i \alpha_{MPC,i}(\Delta^j) \leq \hat{u}_i \leq \varepsilon_i \alpha_{MPC,i}(\Delta^j) \text{ if } \alpha_{MPC,i}(\Delta^j) \geq 0, \quad (7a)$$

$$\varepsilon_i \alpha_{MPC,i}(\Delta^j) \leq \hat{u}_i \leq -\varepsilon_i \alpha_{MPC,i}(\Delta^j) \text{ if } \alpha_{MPC,i}(\Delta^j) \leq 0. \quad (7b)$$

Note that if $\alpha_{MPC,i}(\Delta^j) = 0$, then $\hat{u}_i = 0$. Therefore, in every \mathfrak{B}^η , z appears in \mathbf{R} in a linear fashion; hence, it is easy to re-write \mathbf{R} into the following form:

$$\begin{aligned} \min_c \quad & c^T K c \\ \text{s.t.} \quad & G c \leq W + J^\eta z, \end{aligned} \quad (8)$$

where c is the collection of $(\hat{F}, \hat{\Omega}, \hat{A}, \hat{u}, \beta)$ in vector form and $K \succeq 0$, G , W and J^η are matrices with suitable dimensions.

Note that only J^η depends on η . By [17, Theorem 1.12], for every $\eta \in \{-1, 1\}^{|\mathcal{S}^u|}$, c^* is a continuous and piece-wise affine function of z whenever $z \in \mathfrak{B}^\eta$. Since each \mathfrak{B}^η consists of only linear constraints and the union of all \mathfrak{B}^η 's with $\eta \in \{1, -1\}^{|\mathcal{S}^u|}$ is $\mathbb{R}^{(N+2)n+m}$, one has that c^* is piece-wise affine in z on $\mathbb{R}^{(N+2)n+m}$. Lastly, to show the continuous dependence of c^* on z on $\mathbb{R}^{(N+2)n+m}$, note that since such a dependence holds on every closed set \mathfrak{B}^η , we only need to prove that c^* is unique for every z lying on the boundary shared by different \mathfrak{B}^η 's. This holds trivially as c^* is unique for every $z \in \mathbb{R}^{(N+2)n+m}$, which we have proven above. ■

Notice that Lemma 4.2 implies that \hat{u}^* is globally Lipschitz in z (and hence in the sampled state $f(\Delta^j), \omega(\Delta^j)$, and $\alpha_{MPC}(\Delta^j)$), with $L \triangleq \max_{i \in [1, l]_{\mathbb{N}}} \|F_i\|$ serving as a global Lipschitz constant. Another interesting consequence of this result is that it provides an alternative to directly solving the optimization problem \mathbf{R} . In fact, one can compute and store offline $\{H_i\}_{i=1}^l$, $\{S_i\}_{i=1}^l$, $\{h_i\}_{i=1}^l$, and $\{s_i\}_{i=1}^l$, and then compute \hat{u}^* online using (6). However, this approach faces practical difficulties regarding storage capacity [18], as the number l grows exponentially with system order $m+n$, input size $|\mathcal{S}^u|$, as well as the horizon length N .

2) *Stability and low-pass filter:* Next we introduce the stability and low-pass filters. Note that for any time $t \in (\Delta_j, \Delta_{j+1})$, due to the sampling mechanism, $u_{MPC}(t)$ depends on the old sampled state at time Δ_j , as opposed to the state information at current time t . Since such a lack of update may jeopardize system stability, we cascade a stability filter that depends on the current state after the MPC component to filter out the unstable part in u_{MPC} . The goal of low-pass filter is to simply ensure that the output of the bottom layer is continuous in time. Formally, for every $i \in \mathcal{S}^u$ at any $t \geq 0$, define the stability filter as

$$\begin{aligned} \hat{u}_{MPC,i}(\alpha_{MPC}(t), u_{MPC}(t)) \\ = \text{sat}(u_{MPC,i}(t); \varepsilon_i |\alpha_{MPC,i}(t)|, -\varepsilon_i |\alpha_{MPC,i}(t)|), \end{aligned} \quad (9)$$

and define the low-pass filter as

$$\begin{aligned} \dot{\alpha}_{MPC,i}(t) &= -\frac{1}{T_i} \alpha_{MPC,i}(t) - \omega_i(t) + \hat{u}_{MPC,i}(t), \quad \forall i \in \mathcal{S}^u, \\ \alpha_{MPC,i} &\equiv 0, \quad \forall i \in \mathcal{S} \setminus \mathcal{S}^u. \end{aligned} \quad (10)$$

Note that the low-pass filter model matches the structure in the discretized model (3b). Also, both (9) and (10) can be implemented in a distributed fashion: $\alpha_{MPC,i}$ depends on ω_i and $\hat{u}_{MPC,i}$, and $\hat{u}_{MPC,i}$ only relies on $\alpha_{MPC,i}$ and $u_{MPC,i}$, both of which are local information for node i . For simplicity, we interchangeably use $\hat{u}_{MPC,i}(\alpha_{MPC}(t), u_{MPC}(t))$ and $\hat{u}_{MPC,i}(t)$.

The following result shows the Lipschitz continuity of \hat{u}_{MPC} and points out a condition it satisfies. Later we show that this condition ensures stability of the closed-loop system.

Lemma 4.3: (Lipschitz continuity and stability condition). For the signal \hat{u}_{MPC} defined in (9), \hat{u}_{MPC} is Lipschitz in system state at every sampling time $t = \Delta^j$ with $j \in \mathbb{N}$. Additionally, it holds that

$$\alpha_{MPC,i}(t) \hat{u}_{MPC,i}(t) \leq \varepsilon_i \alpha_{MPC,i}^2(t), \quad \forall t \geq 0, \forall i \in \mathcal{S}. \quad (11)$$

Proof: If $t = \Delta^j$, then since $|\hat{u}_i^*| \leq \varepsilon_i |\alpha_{MPC,i}(\Delta^j)|$ and $u_{MPC,i}(\Delta^j) = \hat{u}_i^*$ for every $i \in \mathcal{S}^u$, by (9), it holds that

$\hat{u}_{MPC,i}(\alpha_{MPC}(t), u_{MPC}(t))|_{t=\Delta_j} = \hat{u}_i^*$. The Lipschitz continuity follows by Lemma 4.2. Condition (11) simply follows by the definition of saturation function. ■

By Lemma 4.3, since \hat{u}_{MPC} is Lipschitz at every sampling time, if the top layer controller is also Lipschitz (which is the case, see Section IV-B), then the solution of the closed-loop system exists and is unique and continuous in time. By (9) and noting that u_{MPC} is piece-wise constant in time, one has \hat{u}_{MPC} is piece-wise continuous, which further implies that α_{MPC} is indeed continuous in time.

Remark 4.4: (Almost independent design of MPC component and stability filter). Note that, regardless of the MPC component output u_{MPC} , the output of the stability filter \hat{u}_{MPC} defined in (9) always meets condition (11). This strong property provides flexibility in the MPC component design and robustness against, e.g., inaccuracy in sampled state measurement, forecasted power injection, as well as system parameters. However, to ensure the Lipschitz continuity in Lemma 4.3, we cast constraint (3f) that shares a same coefficient ε_i in the stability filter (9). To address this aspect, the designs of the MPC component and stability filter are not completely independent. •

Remark 4.5: (Unnecessity of stability filter with continuous sampling MPC component). Our purpose of considering the stability filter here is to ensure that the filtered signal \hat{u}_{MPC} satisfies condition (11). However, if the MPC component can ideally sample the system state in a continuous fashion (as opposed to periodic sampling), then there is no need to additionally add such a stability filter, as pre-filtered signal already satisfies such a condition. In detail, if we define $u_{MPC}(t) = \hat{u}^*(\mathcal{G}, \mathcal{J}^u, \mathcal{J}^\omega, p_i^{fcst}, f(t), \omega(t), \alpha_{MPC}(t))$ for every $t \geq 0$, then due to constraint (3f), one can easily see $\alpha_{MPC,i}(t)u_{MPC,i}(t) \leq \varepsilon_i \alpha_{MPC,i}^2(t), \forall t \geq 0, \forall i \in \mathcal{S}$. Hence, in this scenario, one can safely ignore the stability filter and directly have u_{MPC} as the input of the low-pass filter. •

B. Top layer design through direct feedback

Although the bottom layer control attempts to achieve frequency invariance and attractivity requirements by constraining the predicted frequency trajectory via (3e), it cannot solely guarantee the two requirements. To address this aspect, we construct the top layer control from [9] that is precisely designed to correct potential violations of the frequency requirements by kicking in as the margin of violations gets smaller. Formally, for every $i \in \mathcal{S}^\omega$, let $\tilde{\gamma}_i, \gamma_i > 0$, and $\underline{\omega}_i^{\text{thr}}, \bar{\omega}_i^{\text{thr}} \in \mathbb{R}$ with $\underline{\omega}_i < \underline{\omega}_i^{\text{thr}} < 0 < \bar{\omega}_i^{\text{thr}} < \bar{\omega}_i$. Define the top layer controller α_{DF} as in (12).

Note that the top layer control signal is only available for node with index in \mathcal{S}^ω , and that α_{DF} can be implemented distributedly, in the sense that for each $\alpha_{DF,i}$ with $i \in \mathcal{S}^\omega$ regulated at node i , it only requires its nodal frequency ω_i , aggregated power flow $[D^T]_i f$, power injection p_i , as well as the local bottom layer control signal $\alpha_{MPC,i}$. In addition, we have shown [9] that α_{DF} is locally Lipschitz in its first argument. If the context is clear, we may interchangeably use $\alpha_{DF,i}(x(t), p(t), \alpha_{MPC}(t))$ (resp. $v_i(x(t), \alpha_{MPC}(t), p(t))$) and $\alpha_{DF,i}(t)$ (resp. $v_i(t)$).

C. Closed-loop stability, frequency invariance, and frequency attractivity analysis

With both layers introduced, we are ready to analyze the stability of the closed-loop system and show that it meets the requirements (i)-(iii) in Section III-B. Notice that as we individually introduce each component in the control scheme, we have shown that all components are Lipschitz, and the economic cooperation is encoded in the MPC component; therefore, the requirements (iv) and (v) are met.

Theorem 4.6: (Centralized double-layered control with stability and frequency guarantees). Under Assumption 3.1, if $\varepsilon_i T_i < 1$ for every $i \in \mathcal{S}^u$, then the system (1) with controller defined by (2), (5), (9), (10), and (12) meets requirements (i)-(iii). Furthermore, $\alpha(t)$, $\alpha_{MPC}(t)$, and $\alpha_{DF}(t)$ converge to $\mathbf{0}_n$ as $t \rightarrow \infty$.

Proof: We first consider requirement (iii). Without loss of generality, we can assume that p is constant so that the closed-loop system is time-invariant. Otherwise one can simply consider $t = \bar{t}$ as the initial state. Select the energy function

$$V(f, \omega, \alpha_{MPC}) \triangleq \frac{1}{2}(f - f_\infty)^T(f - f_\infty) + \frac{1}{2}\omega^T M \omega + \frac{1}{2}\alpha_{MPC}^T \alpha_{MPC}$$

After some computations, we obtain

$$\begin{aligned} \dot{V} = & -\omega^T(t)E\omega(t) + \sum_{i \in \mathcal{S}^\omega} \omega_i(t)\alpha_{DF,i}(t) \\ & - \sum_{i \in \mathcal{S}^u} \left(\frac{1}{T_i} \alpha_{MPC,i}^2(t) - \alpha_{MPC,i}(t)\hat{u}_{MPC,i}(t) \right). \end{aligned}$$

Note that by the definition of α_{DF} in (12), $\omega_i(t)\alpha_{DF,i}(t) \leq 0$ holds for every $i \in \mathcal{S}^\omega$ at every $t \geq 0$, in that $\alpha_{DF,i}(t) = 0$ whenever $\underline{\omega}_i^{\text{thr}} \leq \omega_i(t) \leq \bar{\omega}_i^{\text{thr}}$, and $\alpha_{DF,i}(t) \geq 0$ (reps. ≤ 0) if $\omega_i(t) \geq \bar{\omega}_i^{\text{thr}} > 0$ (resp. $\omega_i(t) \leq \underline{\omega}_i^{\text{thr}} < 0$). Therefore, together with condition (11) in Lemma 4.3, we have

$$\dot{V} \leq -\omega^T(t)E\omega(t) - \sum_{i \in \mathcal{S}^u} \left(\frac{1}{T_i} - \varepsilon_i \right) \alpha_{MPC,i}^2(t) \leq 0.$$

The convergence follows by LaSalle's invariance principle. Specifically, $\omega(t)$ and $\alpha_{MPC}(t)$ converge to $\mathbf{0}_n$ (notice that $\alpha_{MPC,i} \equiv 0$ for each $i \in \mathcal{S} \setminus \mathcal{S}^u$). Next we show that $\lim_{t \rightarrow \infty} \alpha_{DF,i}(t) = 0$ for every $i \in \mathcal{S}^\omega$, which implies that $\lim_{t \rightarrow \infty} \alpha_{DF}(t) = \mathbf{0}_n$ as $\alpha_{DF,i} \equiv 0$ for each $i \in \mathcal{S} \setminus \mathcal{S}^\omega$. This simply follows from (12) since $\alpha_{DF,i}(t) = 0$ whenever $\underline{\omega}_i^{\text{thr}} \leq \omega_i(t) \leq \bar{\omega}_i^{\text{thr}}$, where $0 \in (\underline{\omega}_i^{\text{thr}}, \bar{\omega}_i^{\text{thr}})$, and we have shown that $\lim_{t \rightarrow \infty} \omega(t) = \mathbf{0}_n$. The convergence of $\alpha(t)$ follows by its definition (2).

For requirement (i), we have shown in [9] that it is equivalent to asking that for any $i \in \mathcal{S}^\omega$ at any $t \geq 0$,

$$\dot{\omega}_i(t) \leq 0 \text{ if } \omega_i(t) = \bar{\omega}_i, \quad (13a)$$

$$\dot{\omega}_i(t) \geq 0 \text{ if } \omega_i(t) = \underline{\omega}_i. \quad (13b)$$

For simplicity, we only prove (13a), and (13b) follows similarly. Note that by (1b), (2), and (12), one has

$$\begin{aligned} \dot{\omega}_i(t) = & -E_i \omega_i(t) - [D]^T f(t) + p_i(t) + \alpha_i(t) \\ = & -E_i \omega_i(t) - [D]^T f(t) + p_i(t) + \alpha_{MPC,i}(t) + \alpha_{DF,i}(t) \\ = & -v_i(t) + \alpha_{DF,i}(t). \end{aligned}$$

$$\forall i \in \mathcal{S}^\omega, \text{ let } \alpha_{DF,i}(x(t), p(t), \alpha_{MPC}(t)) = \begin{cases} \min\{0, \frac{\tilde{\gamma}_i(\bar{\omega}_i - \omega_i(t))}{\omega_i(t) - \bar{\omega}_i^{\text{thr}}} + v_i(x(t), \alpha_{MPC}(t), p(t))\} & \omega_i(t) > \bar{\omega}_i^{\text{thr}}, \\ 0 & \underline{\omega}_i^{\text{thr}} \leq \omega_i(t) \leq \bar{\omega}_i^{\text{thr}}, \\ \max\{0, \frac{\underline{\gamma}_i(\omega_i - \underline{\omega}_i(t))}{\underline{\omega}_i^{\text{thr}} - \omega_i(t)} + v_i(x(t), \alpha_{MPC}(t), p(t))\} & \omega_i(t) < \underline{\omega}_i^{\text{thr}}, \end{cases} \quad (12a)$$

$$v_i(x(t), \alpha_{MPC}(t), p(t)) \triangleq E_i \omega_i(t) + [D^T]_i f(t) - p_i(t) - \alpha_{MPC,i}(t), \quad (12b)$$

$$\forall i \in \mathcal{S} \setminus \mathcal{S}^\omega, \text{ let } \alpha_{DF,i} \equiv 0. \quad (12c)$$

Now if $\omega_i(t) = \bar{\omega}_i$, then $-v_i(t) + \alpha_{DF,i}(t) = -v_i(t) + \min\{0, v_i(t)\} \leq 0$; hence condition (13a) holds.

Finally, requirement (ii) follows immediately from (i) and (iii). As for any $i \in \mathcal{S}$, ω_i converges to $0 \in (\underline{\omega}_i, \bar{\omega}_i)$, there must exist a finite time t_0 such that $\omega_i(t_0) \in [\underline{\omega}_i, \bar{\omega}_i]$, which, by frequency invariance, implies that $\omega_i(t) \in [\underline{\omega}_i, \bar{\omega}_i]$ at any $t \geq t_0$. ■

Remark 4.7: (Control framework without bottom layer). We have shown in [9] that even if one only implements the first-layer controller (i.e., $\alpha_{MPC} \equiv \mathbf{0}_n$, leading to $\alpha = \alpha_{DF}$), the closed-loop system still meets all requirements except for the economic cooperation. Such a lack of cooperation can be seen from two aspects. First, since α_{DF} is only available for nodes in \mathcal{S}^ω , those in $\mathcal{S}^u \setminus \mathcal{S}^\omega$ do not get involved in controlling frequency transients. Second, the first-layer control is a non-optimization-based state feedback, where each $\alpha_{DF,i}$ with $i \in \mathcal{S}^\omega$ is merely in charge of controlling transient frequency for its own node i . •

Since the centralized doubled-layered control scheme already meets requirements (i)-(v), in the next section, we deal with the remaining distributed computation requirement.

V. CONTROLLER DECENTRALIZATION THROUGH NETWORK DIVISION

Going over the double-layered design in the previous section, it is worth noticing that the only component of the controller that requires global information is the MPC component, all the others being local in nature. In this section, we propose a distributed double-layered controller design that addresses this point. The general idea is to split the computation of the MPC component across different regions, and have each region determine its own MPC component based on its regional state and regional forecasted power information.

We split the network into regions so that each controlled node is contained in exactly one region. Formally, let $\{\mathcal{G}_\beta = (\mathcal{S}_\beta, \mathcal{E}_\beta)\}_{\beta \in [1, d]_{\mathbb{N}}}$ be induced subgraphs of \mathcal{G} such that

$$\mathcal{S}^u \subseteq \bigcup_{\beta=1}^d \mathcal{S}_\beta, \quad (14a)$$

$$\mathcal{S}_\eta \cap \mathcal{S}_\beta \cap \mathcal{S}^u = \emptyset, \quad \forall \eta, \beta \in [1, d]_{\mathbb{N}} \text{ with } \eta \neq \beta. \quad (14b)$$

For each subgraph \mathcal{G}_β , let $\mathcal{S}_\beta^u \triangleq \mathcal{S}^u \cap \mathcal{S}_\beta$ (resp. $\mathcal{S}_\beta^\omega \triangleq \mathcal{S}^\omega \cap \mathcal{S}_\beta$) denote the collection of controlled node indexes (resp. nodes indexes with transient frequency requirements) within \mathcal{G}_β . Let $(f_\beta, \omega_\beta, \alpha_{MPC,\beta}) \in \mathbb{R}^{2|\mathcal{S}_\beta| + |\mathcal{E}_\beta^f|}$ be the collection of states in \mathcal{G}_β . Let $p_{t,\beta}^{fcst} : [t, t + \tilde{t}] \rightarrow \mathbb{R}^{|\mathcal{S}_\beta|}$ be the

forecasted power injection for every node in \mathcal{G}_β starting from time t to \tilde{t} seconds later. Note that the dynamics of \mathcal{G}_β is not completely determined by $(f_\beta, \omega_\beta, \alpha_{MPC,\beta})$ due to its interconnection with other parts of the network outside \mathcal{G}_β through transmission lines with $i \in \mathcal{S}_\beta$ and $j \in \mathcal{S} \setminus \mathcal{S}_\beta$ (equivalently, with $(i, j) \in \mathcal{E}_\beta^f$). Instead of considering the flows f_{ij} 's of these transmission lines as states for \mathcal{G}_β , we model them as exogenous power injections. Formally, denote for every $i \in \mathcal{S}_\beta$,

$$p_{t,\beta,i}^{fcst,f}(\tau) \triangleq \sum_{\substack{j:j \rightarrow i \\ (j,i) \in \mathcal{E}_\beta^f}} f_{ji}(t) - \sum_{\substack{j:i \rightarrow j \\ (i,j) \in \mathcal{E}_\beta^f}} f_{ij}(t), \quad \forall \tau \in [t, t + \tilde{t}] \quad (15)$$

as the forecasted exogenous power injection acting on node i caused by transmission lines in \mathcal{E}_β^f , where $\{j : j \rightarrow i\}$ is the shorthand notation for $\{j : j \in \mathcal{N}(i) \text{ and } j \text{ is the positive end of } (i, j)\}$. For simplicity, here we take the forecasted value starting from time t to be constant within the time interval $[t, t + \tilde{t}]$. Denote by $p_{t,\beta}^{fcst} : [t, t + \tilde{t}] \rightarrow \mathbb{R}^{|\mathcal{S}_\beta|}$ the collection of all $p_{t,i}^{fcst}$'s with $i \in \mathcal{S}_\beta$, and let $\bar{p}_{t,\beta}^{fcst} \triangleq p_{t,\beta}^{fcst} + p_{t,\beta}^{fcst,f}$ be the overall forecasted power injection. We illustrate these definitions in an example.

Example 5.1: (A network division in IEEE 39-bus network). Fig. 2 shows a network division example with $\mathcal{S}^\omega = \{30, 31, 32, 37\}$ and $\mathcal{S}^u = \{3, 7, 25, 30, 31, 32, 37\}$. The set \mathcal{S}^u consists of all nodes in \mathcal{S}^ω and all nodes capable of adjusting their loads and within two hops of a node in \mathcal{S}^ω . We split the network into three regions ($d = 3$) satisfying (14). Each region \mathcal{G}_β contains the two-hop neighborhood for every node in \mathcal{S}_β^ω . We denote by \mathcal{G}_1 the upper left region in Fig. 2 and use it to illustrate related definitions. In \mathcal{G}_1 , one has $\mathcal{S}_1 = \{1, 2, 3, 25, 26, 30, 37\}$, $\mathcal{S}_1^\omega = \{30, 37\}$, $\mathcal{S}_1^u = \{3, 25, 30, 37\}$, $\mathcal{E}_1 = \{(1, 2), (2, 30), (2, 25), (3, 25), (25, 37), (26, 37)\}$, and $\mathcal{E}_1^f = \{(1, 39), (3, 4), (3, 18), (26, 27), (26, 28), (26, 29)\}$. For every $i \in \mathcal{S}_1$, one can compute $p_{t,\beta,i}^{fcst,f}$ by (15), and it is easy to see that $p_{t,\beta,i}^{fcst,f} \equiv 0$ for $i \in \{2, 3, 25, 30, 37\}$, as these nodes are not ends of any edge in \mathcal{E}_1^f . •

The key idea of designing the distributed MPC component is to consider each region as an single network and separately implement the centralized MPC on it. Formally, for every $\beta \in [1, d]_{\mathbb{N}}$, let $\{\Delta_\beta^j\}_{j \in \mathbb{N}}$ be its sampling sequence. For every $i \in \mathcal{S}^u$, select the unique β such that $i \in \mathcal{S}_\beta$, and at every

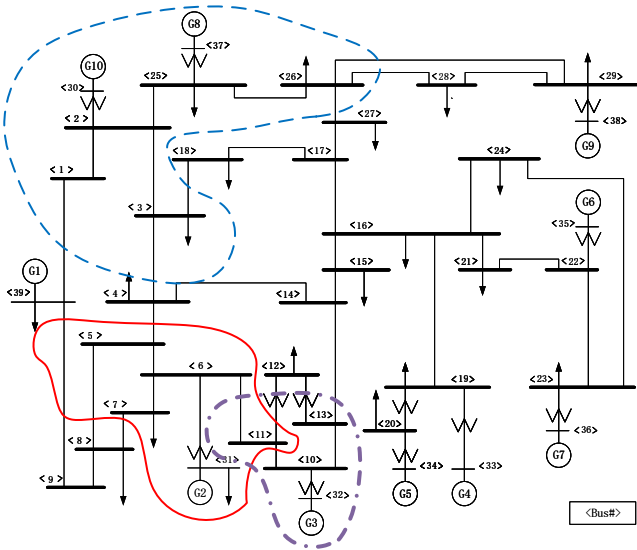


Fig. 2. IEEE 39-bus power network.

$t \in [\Delta_\beta^j, \Delta_\beta^{j+1})$ with $j \in \mathbb{N}$, let

$$u_{MPC,i}(t) = \hat{u}_i^*(\mathcal{G}_\beta, \mathcal{J}_\beta^u, \mathcal{J}_\beta^\omega, \bar{p}_{\Delta^j, \beta}^{fcst}, f_\beta(\Delta^j), \omega_\beta(\Delta^j), \alpha_\beta(\Delta^j)). \quad (16)$$

Compared to the centralized MPC in (5), the distributed version (16) transforms all global information, including network topology, forecasted power injection and system state, into local information. Their structural difference is that, in the distributed MPC, the overall forecasted power injection $\bar{p}_{\Delta^j, \beta}^{fcst}$ includes an additional term (15) to account for the interconnected dynamics between the region of interest and the rest of the network. Next, we characterize the closed-loop stability and performance of the system under the distributed controller.

Proposition 5.2: (Distributed double-layered control with stability and frequency guarantee). Under Assumption 3.1 and assume that $\varepsilon_i T_i < 1$ for every $i \in \mathcal{J}^u$, system (1) with controller defined by (2), (9), (10), (12), and (16) meets requirements (i)-(iii). Furthermore, $\alpha(t)$, $\alpha_{MPC}(t)$, and $\alpha_{DF}(t)$ converge to $\mathbf{0}_n$ as $t \rightarrow \infty$.

The proof is exactly the same as that of Theorem 4.6, and is omitted.

VI. SIMULATIONS

Here, we illustrate the performance of the distributed controller in the IEEE 39-bus power network described in Fig. 2. All parameters in the network model (1) are taken from the Power System Toolbox [19]. We assign a small rotational inertia $M_i = 0.1$ to all non-generator nodes for simplicity. Let $\bar{\omega}_i = -\underline{\omega}_i = 0.2Hz$, so that the safe frequency region is $[59.8Hz, 60.2Hz]$. To set up the distributed MPC component (16), we select $\tilde{t} = 2s$ and $T = 0.02$, so that the predicted step $N = 100$; $\varepsilon_i = 1.9$ and $T_i = 0.5$ for every $i \in \mathcal{J}^u$; $c_i = 1$ if $i \in \mathcal{J}^\omega$, while $c_i = 4$ if $i \in \mathcal{J}^u \setminus \mathcal{J}^\omega$; $d = 100$; $\{\Delta_\beta^j\}_{j \in \mathbb{N}} = \{j\}_{j \in \mathbb{N}}$ for every $\beta \in [1, d]_{\mathbb{N}}$, i.e., in each region, the MPC component samples and updates its output every 1s; $p_i^{fcst}(\tau) = p(\tau)$ for every $\tau \in [t, t + \tilde{t}]$, i.e., the forecasted power injection is precise. To set up the top

layer controller (12), let $\tilde{\gamma}_i = \underline{\gamma}_i = 1$ and $\bar{\omega}_i^{\text{thr}} = -\underline{\omega}_i^{\text{thr}} = 0.1Hz$ for every $i \in \mathcal{J}^\omega$.

We first show that the distributed controller defined by (2), (9), (10), (12), and (16) is able to maintain the targeted nodal frequencies within the safe region without changing the open loop equilibrium. We disturb all non-generator nodes by some time-varying power injections. In detail, for every $i \in [1, 29]_{\mathbb{N}}$, let $p_i(t) = (1 + \delta(t))p_i(0)$, where

$$\delta(t) = \begin{cases} 0.2 \sin(\pi t / 50) & \text{if } 0 \leq t \leq 25 \\ 0.2 & \text{if } 25 < t \leq 125 \\ 0.2 \sin(\pi(t - 100) / 50) & \text{if } 125 < t \leq 150 \\ 0 & \text{if } 150 < t \end{cases}$$

The deviation term $\delta(t)p_i(0)$ first drops down at a relatively fast rate and then remains steady for a long time period, finally converges to 0. We have chosen this scenario to test the capability of the controller against both fast and slow time-varying power injection disturbances.

For simplicity, in the following we focus on the state and control input trajectories in the left-top region in Fig. 2. Fig. 3(a) shows the open-loop frequency responses of node 30 and 37, which have transient frequency requirements. The two nodes have almost the same overlapping trajectories that both exceed the safe lower frequency bound $59.8Hz$. As a comparison, in Fig. 3 (b), with the distributed controller, their frequency responses stay within the safe region, and also gradually come back to $60Hz$ after the disturbance disappears. Given the selected coefficients $c_3 = c_{25} = 1$ and $c_{30} = c_{37} = 4$ in the optimization problem (3), the controller tends to use α_3 and α_{25} more than α_{30} and α_{37} , and this is reflected in the control trajectories in Fig. 3(c). Fig. 3(d) shows the control trajectories for the non-optimization-based controller proposed in [9]. Compared with those in Fig. 3(c), α_{30} and α_{37} do not have a similar trend, and the control actions at node 3 and 25 have to be disabled, cf. Remark 4.7.

We then come back to our distributed controller and further focus on the control signal at node 30 by decomposing α_{30} into its bottom layer output $\alpha_{MPC,30}$ and top layer output $\alpha_{DF,30}$. As shown in Fig. 4(a), $\alpha_{MPC,30}$ is responsible for the larger share in the overall control signal α_{30} , whereas $\alpha_{DF,30}$ only slightly tunes α_{30} . However, if we reduce the penalty d_{30} from 100 to 10, in Fig. 4(b), the dominance of $\alpha_{MPC,30}$ decreases, in accordance with our discussion in Remark 4.1.

Lastly, to verify that the proposed controller meets frequency attractivity requirement, we consider a case where the initial frequency is outside the safe region and see how the controller force the frequency back to the region. To do so, we disable in the setup above the distributed controller for the first 30s. In Fig. 5(a), one can see that the frequency of node 30 quickly recovers once we switch on the distributed controller. Fig. 5(b) shows the control signal of node 30. Note that, after transients, $\alpha_{MPC,30}$ still dominates the overall control signal.

VII. CONCLUSIONS

We have proposed a distributed transient frequency control framework for power networks that preserves the asymptotic

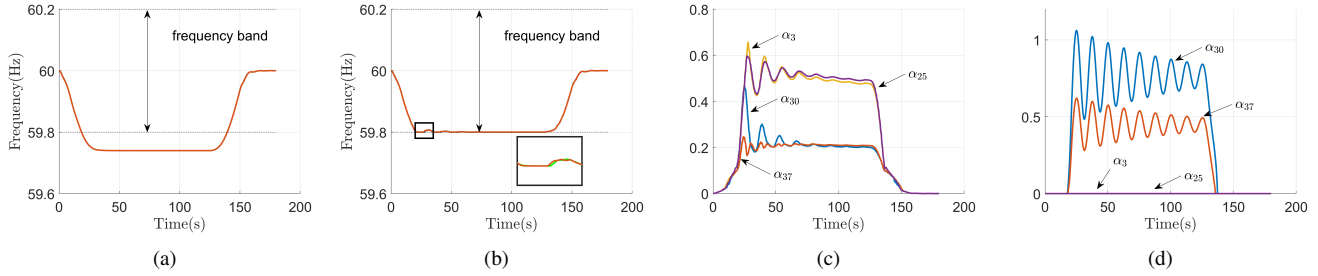


Fig. 3. Frequency and control input trajectories with and without distributed transient frequency control. Plot (a) shows the open-loop frequency responses at node 30 and 37, both exceeding the lower safe bound. With the distributed control, in plot (b), both stay inside the safe region. Plot (c) shows the corresponding control trajectories, where overall control cost $\sum_{i=3,25,30,37} \int_0^{200} c_i \alpha_i^2(\tau) d\tau = 97.8$. Plot (d) shows the control trajectories with bottom layer disabled, where the overall control cost is 363.5.

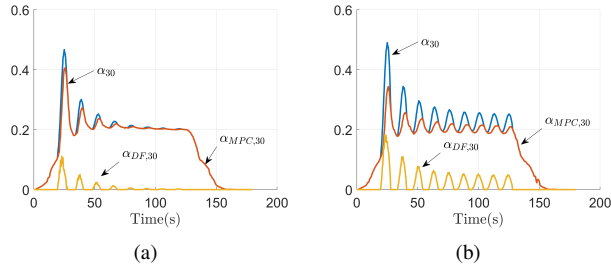


Fig. 4. Control signal decomposition at node 30 with different d_{30} . In plot (a), with $d_{30} = 100$, the bottom layer action dominates the total input. Such a dominance diminishes as we reduce d_{30} to 10, cf. plot (b).

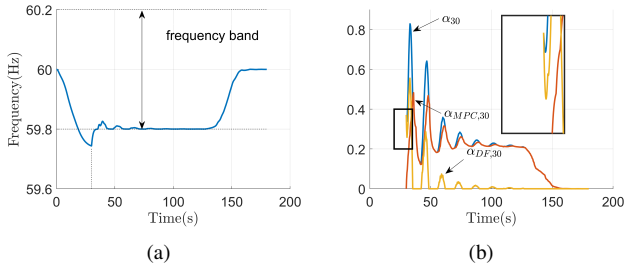


Fig. 5. Frequency and control input trajectories at node 30 with controller available after $t = 30$ s. In plot (a), the frequency gradually comes back to the safe region after the controller kicks in. Plot (b) shows the control signals.

stability of the network and at the same time, guarantees safe frequency interval invariance and attractivity for targeted nodes. The controller possesses a double-layered structure, with the bottom layer periodically sampling the state and allocating control signals over a local region in a receding horizon fashion. The top layer slightly tunes the bottom layer signal in order to provably enforce frequency invariance and attractivity guarantees. Implemented over a network partition, both layers rely on local state and power injection information. Future work will investigate the extension of the results to nonlinear swing dynamics, the optimal selection of sampling sequences in the bottom layer control design, the analysis of the performance trade-offs of the parameter selections, and the designs of distributed control schemes that do not rely on network partitions.

REFERENCES

- [1] N. W. Miller, K. Clark, and M. Shao, "Frequency responsive wind plant controls: Impacts on grid performance," in *IEEE Power and Energy Society General Meeting*, Detroit, MI, Oct. 2011, electronic proceedings.
- [2] F. Milano, F. Dörfler, G. Hug, D. J. Hill, and G. Verbič, "Foundations and challenges of low-inertia systems," in *Power Systems Computation Conference*, Dublin, Ireland, June 2018, electronic proceedings.
- [3] H. D. Chiang, *Direct Methods for Stability Analysis of Electric Power Systems: Theoretical Foundation, BCU Methodologies, and Applications*. John Wiley and Sons, 2011.
- [4] F. Dörfler, M. Chertkov, and F. Bullo, "Synchronization in complex oscillator networks and smart grids," *Proceedings of the National Academy of Sciences*, vol. 110, no. 6, pp. 2005–2010, 2013.
- [5] D. Lee, L. Aolaritei, T. L. Vu, and K. Turitsyn, "Robustness against disturbances in power systems under frequency constraints," *arXiv preprint arXiv:1803.00817*, 2018.
- [6] T. S. Borsche, T. Liu, and D. J. Hill, "Effects of rotational inertia on power system damping and frequency transients," in *IEEE Conf. on Decision and Control*, Osaka, Japan, 2015, pp. 5940–5946.
- [7] P. Kundur, *Power System Stability and Control*. McGraw-Hill, 1994.
- [8] A. Alam and E. Makram, "Transient stability constrained optimal power flow," in *IEEE Power and Energy Society General Meeting*, Montreal, Canada, Jun. 2006, electronic proceedings.
- [9] Y. Zhang and J. Cortés, "Distributed transient frequency control in power networks," in *IEEE Conf. on Decision and Control*, Miami Beach, FL, Dec. 2018, to appear.
- [10] —, "Transient frequency control with regional cooperation for power networks," in *IEEE Conf. on Decision and Control*, Miami Beach, FL, Dec. 2018, to appear.
- [11] F. Bullo, J. Cortés, and S. Martínez, *Distributed Control of Robotic Networks*, ser. Applied Mathematics Series. Princeton University Press, 2009, electronically available at <http://coordinationbook.info>.
- [12] N. Biggs, *Algebraic Graph Theory*, 2nd ed. Cambridge University Press, 1994.
- [13] A. R. Bergen and D. J. Hill, "A structure preserving model for power system stability analysis," *IEEE Transactions on Power Apparatus and Systems*, vol. 100, no. 1, pp. 25–35, 1981.
- [14] A. Pai, *Energy Function Analysis for Power System Stability*. New York: Springer, 1989.
- [15] C. Zhao, U. Topcu, N. Li, and S. H. Low, "Design and stability of load-side primary frequency control in power systems," *IEEE Transactions on Automatic Control*, vol. 59, no. 5, pp. 1177–1189, 2014.
- [16] A. R. Bergen and V. Vittal, *Power System Analysis*. Upper Saddle River, NJ: Prentice Hall, 2000.
- [17] F. Borrelli, *Constrained Optimal Control of Linear and Hybrid Systems*. New York: Springer, 2003.
- [18] J. B. Rawlings and D. Q. Mayne, *Model predictive control: theory and design*. Madison, WI: Nob Hill Pub. cop., 2009. [Online]. Available: <http://opac.inria.fr/record=b1133273>
- [19] K. W. Cheung, J. Chow, and G. Rogers, *Power System Toolbox, v 3.0*. Rensselaer Polytechnic Institute and Cherry Tree Scientific Software, 2009.